Phase transitions and phase diagrams of K and Cs overlayers on a reconstructed and unreconstructed Cu(110) surface

W. C. Fan and A. Ignatiev
Department of Physics, University of Houston, Houston, Texas 77004
(Received 9 December 1987; revised manuscript received 5 February 1988)

Low-energy electron-diffraction experiments have been carried out to study the phase transitions of K and Cs on a Cu(110) surface and the copper substrate reconstruction under adsorption within the temperature range between 80 and 400 K. The K and Cs adatoms on an 80-K Cu(110) substrate form quasihexagonally (QH) ordered structures when the nearest atomic spacing between the adatoms reaches the value $\simeq 8$ Å (coverage $\Theta \simeq 0.17$). The disordering transition temperature of the QH structures for both K and Cs overlayers increases as coverage increases. The substrate surface reconstruction induced by the K and Cs overlayers starts at $T \simeq 150$ K and $\Theta \simeq 0.05$. The relationships between the QH phases of alkali overlayers and the (1×3) and (1×2) phases of the surface reconstruction are described quantitatively in phase diagrams for the K and Cs systems. A continuous phase transition ($T_c > 260$ K) from a well-ordered (1×2)-reconstructed surface to the (1×3)-reconstructed surface is also described as a function of excess K or Cs deposition ($\Delta\Theta$).

I. INTRODUCTION

Substrate surface reconstruction is an interesting phenomenon observed on a variety of surfaces. A number of substrate surface reconstructions induced by adsorbates have been reported recently, including the reconstruction of fcc-metal (110) surfaces[1-3] and bcc-metal (100) and (110) surfaces.[4-6] Theoretical efforts have also been devoted to the explanation of the driving force for surface reconstruction by invoking a surface-phonon-mode-softening model.[7] One of the interesting reconstructions in these metal systems is the (1×2) reconstruction observed on many fcc (110) metal surfaces.[1-3] Low-energy electron-diffraction (LEED) dynamical calculations[1,3] indicate that the (1×2) reconstruction is consistent with the "missing-row" model or the "row-paring" model, but not the "sawtooth" model. Recent theoretical calculations for Pt(110) using the embedded-atom method have also shown that the (1×2) reconstruction favors the "missing-row" structure over the "sawtooth" structure.[8] On the other hand, scanning tunneling microscope (STM) studies of a (1×2)-reconstructed Ni(110) surface indicate a "(5×2)"-like domain structure,[9] showing that the exact surface topology and atomic structure for the (110) surface (1×2) reconstruction may be much more complicated than the simple models indicate.

Within the fcc (110) system, substrate reconstruction has also been induced by alkali-metal adsorption on Ag(110) and Cu(110).[10] As pointed out there, the Cu(110) surface reconstruction was similar to Ag(110). However, the details of the Cu(110) surface reconstruction have not been published. In this paper we describe some details of the surface reconstruction of Cu(110) under Cs and K adsorption. In addition, we describe the phase transitions and phase diagrams of Cs and K on Cu(110) surface through measurement of LEED intensities and diffraction-beam profiles as a function of temperature and coverage. It will be shown that the Cu(110) surface reconstruction is strongly dependent on the temperature and the coverage.

II. EXPERIMENTAL

The experiments were carried out in an ultrahigh-vacuum (UHV) chamber with a four-grid LEED optics as described previously.[11-13] The intensities of LEED beams and the beam profiles were measured from the LEED optics with video camera interfaced to a personal computer. The Cu single-crystal sample with a (110) surface was polished with Al_2O_3 polishing paste and then mounted onto a manipulator with capabilities of heating and cooling in UHV. The surface was cleaned by cycles of Ar-ion bombardment and annealing until there was no indication of impurities in the Auger electron spectrum (AES), and the LEED pattern showed sharp, high-contrast diffraction beams after annealing. The temperature was measured by a Chromel-Alumel thermocouple calibrated at 80 K. The alkali-metal sources were Saes-Getter thermal cells located at about 12 cm away from the sample. The evaporation was monitored by AES measurements and by the observation of the LEED patterns. The Cs and K evaporation rates were controlled at about 0.02 ML/min (one monolayer = 1 ML $= 2.7\times 10^{14}$ atom/cm^2 for Cs, 1 ML $= 3.7\times 10^{14}$ atom/cm^2 for K). The vacuum chamber was maintained at better than 3×10^{-10} Torr for the period of the experiments.

III. RESULTS AND DISCUSSIONS

A. K and Cs overlayers on the unreconstructed Cu(110) surface

The evaporation of K onto the Cu(110) surface at 80 K resulted in a disordered structure of K at coverage

$\Theta < 0.17$. Θ is defined as the ratio of the number of adatoms to the number of substrate atoms per unit area, with an accuracy of ± 0.01 determined by LEED and AES. As a result of further evaporation of K ($\Theta > 0.17$), the potassium overlayer formed a quasihexagonal (QH) structure at 80 K as shown in Fig. 1(a). As the coverage increased, the separation, 2Θ in the [10] direction of the overlayer beams [$(\pm\Theta\ \frac{1}{2})$ in Fig. 2(a)] increased as a function of coverage Θ. The labeling of the overlayer beams with Θ means that the beams separation in the [10] direction is just equal to twice the coverage, similar to that in the K/Ni(110) system.[14,15] The separation of the overlayer beams in [01] direction, however, remained constant with increasing coverage as shown in Figs. 1 and 2(a). The change in the diffraction pattern (Fig. 1) implies a continuous compression of the potassium atomic spacing in the [10] direction [Fig. 2(b)] under increased K exposure.

Evaporation of Cs onto Cu(110) resulted in LEED patterns similar to those for potassium. The QH structure is also observed for a Cs overlayer on the 80-K Cu(110) surface. Such behavior has also been seen for inert-gas adsorption on Cu(110) (Refs. 16 and 17) and alkali-metal adsorption on other fcc (110) metal surfaces.[14,15]

According to the diffraction patterns, the overlayer interatomic spacings at maximum coverage are 4.3 Å for K (about 5% smaller than bulk potassium interatomic spacing), and 4.7 Å for Cs (about 10% smaller than that in bulk Cs). The decrease in the interatomic spacing is consistent with the previous results for alkali-metal overlayers on graphite (0001) and Cu(111) surfaces.[11–13] The weak streak of diffraction intensity between the (01) beam and (0−1) beam (Fig. 1) is believed to be the result of a local reconstruction of a portion of the substrate surface, which may be related to surface defects. This diffraction streak will be discussed more later.

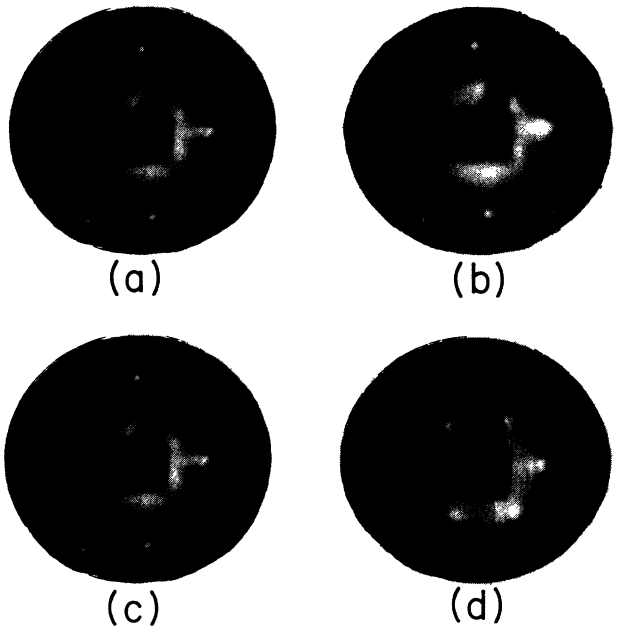

FIG. 1. LEED patterns of the quasihexagonal structure phase (QH) of potassium on the 80-K Cu(110) surface at $E = 82$ eV except (d) at $E = 84$ eV. (a) $\Theta = 0.20$; (b) $\Theta = 0.25$; (c) $\Theta = 0.50$; (d) $\Theta = 0.6$. (d) is the pattern for the minimal K interatomic spacing.

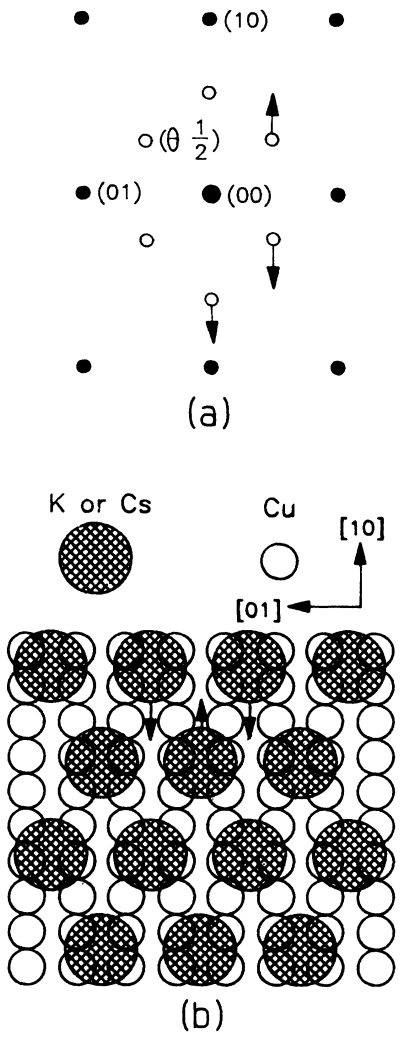

FIG. 2. (a) The schematic LEED pattern of the quasihexagonal structure phase of potassium or cesium on the 80-K Cu(110) surface. The arrows denote the direction of motion of the overlayer beams as coverage increases. (b) A proposed structure of the quasihexagonal phase on the unreconstructed Cu(110) surface.

The order-disorder transition of the QH-phase overlayer has been studied through the measurement of the intensity of the $(\Theta\ \frac{1}{2})$ beam and the beam width along the [10] direction as a function of temperature and coverage (Figs. 3 and 4). The measurements in Fig. 3 are taken from the Cu(110) surface after deposition of cesium onto the 80 K surface. As temperature increases, the intensities of the overlayer beams gradually decrease. As the temperature approaches the disordering transition temperature [which is defined as the inflection point in the intensity-temperature curve (Fig. 3)], the intensities start

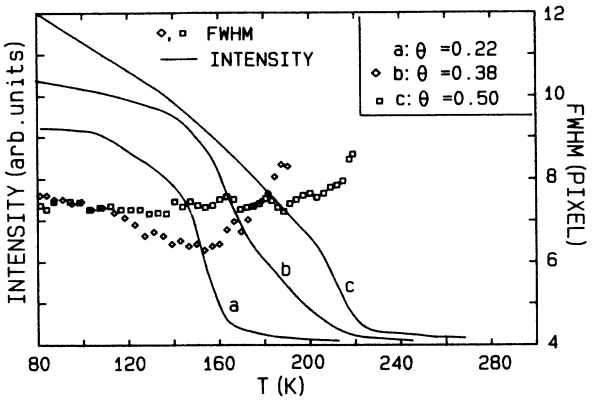

FIG. 3. The LEED intensities and the FWHM's of the cesium overlayer beam ($\Theta \frac{1}{2}$) of the quasihexagonal structure as a function of temperature and coverage. The FWHM's are measured along the [10] direction. 1 pixel$=4.8\times10^{-3}$ (Å)$^{-1}$.

to drop dramatically. The disordering transition temperature (Fig. 3) increases significantly with Cs coverage. At temperatures beyond this transition temperature, the diffracted intensity is still decreasing until the overlayer is completely disordered. Within this temperature region, from the inflection point to that of the completely disordered overlayer, the overlayer is in a short-range-ordered quasihexagonal structure as later noted in the phase diagrams.

The change in the beam widths versus temperature is quite noticeable. At the lower coverage ($\Theta<0.4$), before the saturation of the interatomic spacing in the overlayer, the full width at half maximum (FWHM) of the first-order overlayer beam first decreases at 120 K (as shown in Fig. 4 for $\Theta=0.38$), and then increases continuously near the disordering transition temperature until the overlayer is completely disordered. The decrease of the beam width indicates a transition of the overlayer to a better ordered phase and is believed to result from the decrease of dislocations and defects (or "immobile gas") (Refs. 12 and 18) in the overlayer. This phenomenon has already been observed for the alkali metals on the Cu(111) surface[12,13] but is now more obvious. As a result of the decrease of the "immobile gas" in the overlayer, the interatomic spacing in the overlayer decreases about 2%. At higher coverage ($\Theta>0.4$), after the saturation of the interatomic spacing, the FWHM of the Cs overlayer beam does not decrease at $T>120$ K as shown in Fig. 3 for $\Theta=0.5$.

The order-disorder phase transition behavior of the potassium overlayer on Cu(110) is almost the same as that of the cesium overlayer except for a transition to QH phase at high coverage ($\Theta>0.5$) and high temperature (~360 K). As shown in Fig. 4(a), the LEED intensity of the overlayer beam slightly increases at $T\simeq120$ K while the beam FWHM decreases significantly. The beam width also increases near the disordering transition temperature similar to the case for cesium (Fig. 3). Figure 4(b) shows the beam intensity profiles at several temperatures. It is easy to see that the beam profiles shift towards the [10] direction with increasing temperature while the FWHM decreases. After a drastic drop at $T\simeq250$ K, the intensity increases a small amount at $T>260$ K, indicating an overlayer reordering before going to a completely disordered phase ($T>360$ K). This disordering and reordering of the overlayer at high coverage ($\Theta\simeq0.5$) results from substrate (1×3) reconstruction to be discussed in Sec. II B.

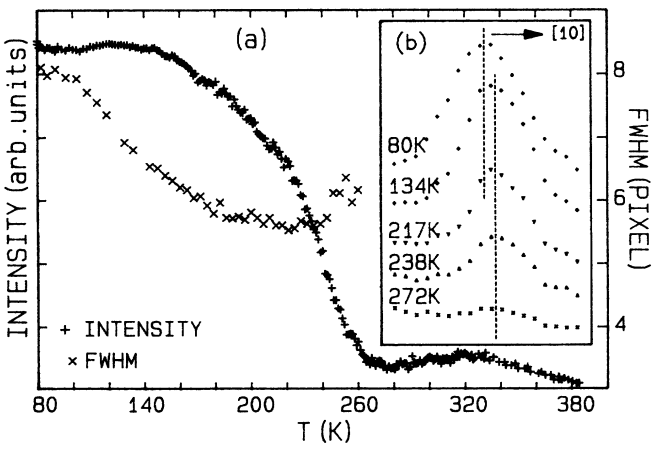

FIG. 4. (a) The LEED intensity and FWHM, and (b) the beam intensity profiles, of the potassium overlayer beam ($\Theta \frac{1}{2}$) of the quasihexagonal structure at coverage $\Theta\simeq0.58$ as a function of temperature. 1 pixel$=4.8\times10^{-3}$ (Å)$^{-1}$.

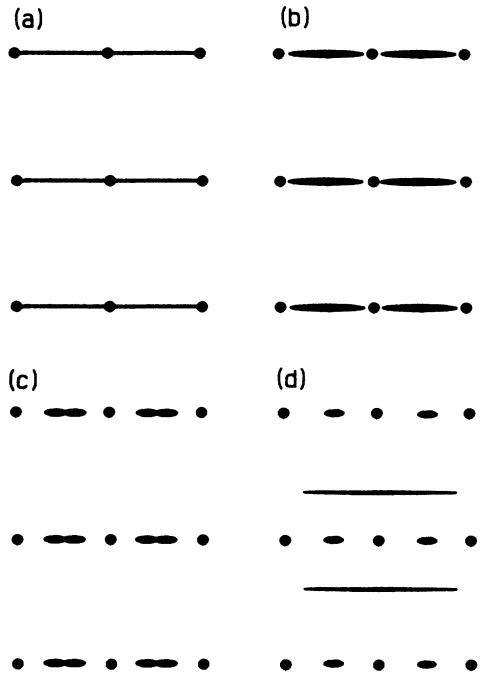

FIG. 5. A series of schematic LEED patterns resulting from the increase of K or Cs coverage on the room-temperature Cu(110) surface. (a) $\Theta\simeq0.05$, (b) $\Theta\simeq0.08$, (c) $\Theta\simeq0.12$, (d) $\Theta\simeq0.25$.

B. Reconstruction of the Cu(110) surface

The evaporation of potassium or cesium onto the room-temperature Cu(110) surface resulted in a sequence of changes in LEED pattern as shown in Fig. 5. As the coverage increased ($\Theta \geq 0.04$), a streak diffraction pattern gradually appeared as shown in Fig. 5(a). At a coverage of $\Theta \simeq 0.12$, the streaks in the diffraction pattern became spotty and the intensity modulated by a (1×3) superstructure [Fig. 5(c)]. This (1×3) phase changed to a (1×2) pattern with additional streaks near the $(\pm\frac{1}{2}0)$ positions, as shown in Fig. 5(d). As coverage further increased ($\Theta > 0.14$), the streaks were clearer and the separation of the streaks increased. However, the (1×2) beams were still elliptical [Fig. 5(d)]. After the coverage reached above 0.3, the (1×2) phase changed back to the (1×3) phase and the additional streaks became weaker and broader in [10] direction.

A similar sequence of changes in the diffraction pattern with increasing coverage has also observed for alkali metals on other fcc (110) surfaces[14,15] at room temperature.

The streak pattern [Fig. 5(a)] is believed to be a result of the surface lattice reconstruction in the [01] direction. These streaks in Fig. 5(a) are equivalent though much clearer and more intense than the streaks from the 80 K substrate mentioned in Sec. II A, thus, the weak streaks in Fig. 1 are only a local reconstruction of a small portion of the surface probably related to surface defects.

The (1×2) phase is a long-range-ordered surface reconstruction with an atomic structure probably of the "row-paring" model or the "missing-row" model.[3] The additional streaks in the (1×2) LEED pattern [Fig. 5(d)] are due to diffraction from the alkali-metal overlayer, indicating that the alkali-metal atoms on the surface are quasi-long-range-ordered within each row and disordered between the rows. Figure 6 shows a possible structure of the alkali atoms, that is a "row" structure of a alkali overlayer on a "missing-row" (1×2) reconstructed surface.

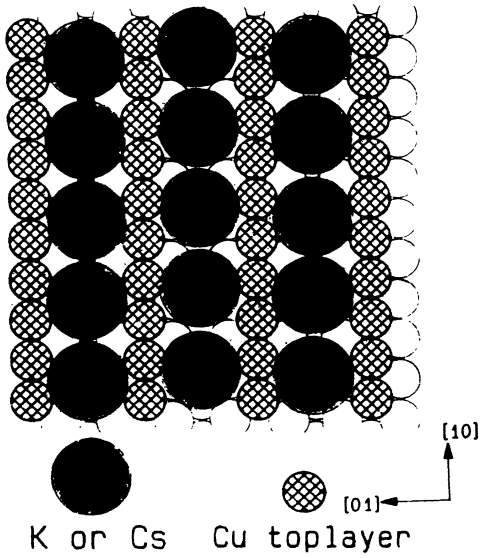

FIG. 6. A possible structure for the (1×2) LEED pattern with additional streaks [Fig. 5(d)], with a (1×2) "missing-row" reconstructed surface and a "row" structure of the alkali-metal overlayer.

Further investigation of the surface reconstruction has been undertaken through the measurements of the LEED intensities at particular positions in reciprocal space as a function of temperature.

Figure 7 shows the measurements of the intensities at the $(0\frac{1}{2})$ and the positions $(0\frac{2}{3})$ versus temperature, after deposition of cesium onto the 80-K Cu(110) surface. With increasing temperature, the LEED intensities start to increase at a temperature $T \simeq 150$ K, as shown in Fig. 7. This temperature is called the substrate reconstruction

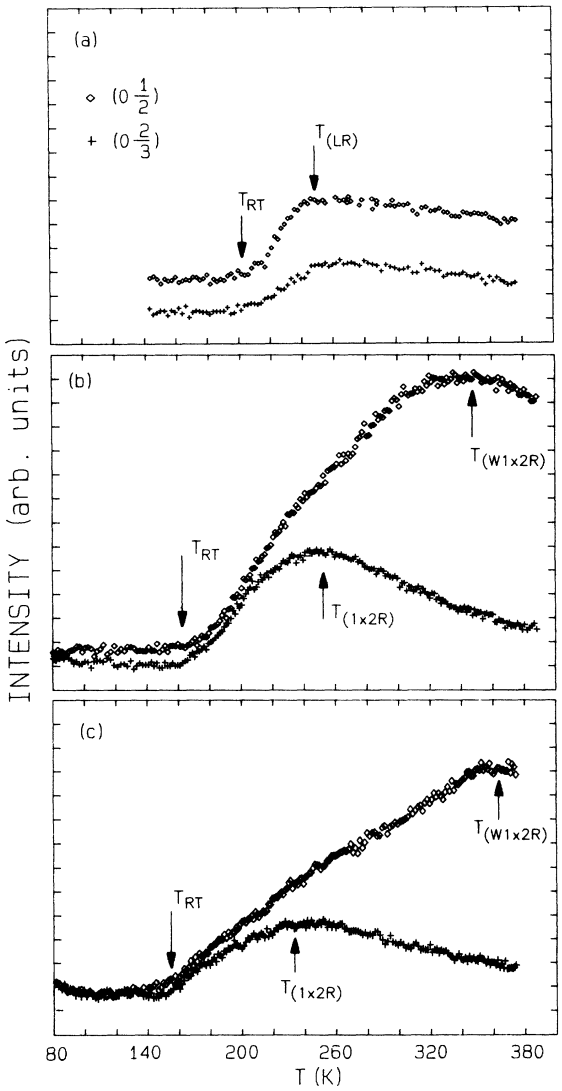

FIG. 7. The LEED intensities at the $(0\frac{1}{2})$ and the $(0\frac{2}{3})$ positions as a function of temperature and Cs coverage. (a) $\Theta = 0.10$, (b) $\Theta = 0.18$, (c) $\Theta = 0.22$. T_{RT} is the substrate reconstruction temperature. $T_{(LR)}$ is the temperature to reach the stable local reconstruction. $T_{(1\times2R)}$ is the temperature of the (1×2) reconstruction. $T_{(W1\times2R)}$ is the temperature to reach a well-ordered (1×2) reconstruction.

temperature (T_{RT}) in later discussions. The increase of the LEED intensities above T_{RT} results from a transition to the streak pattern [Fig. 5(a)]. A similar surface reconstruction behavior has been also observed for Cs on Ag(110) surface.[19] It has been shown there that this local surface reconstruction is associated with a work function shift at T_{RT}.

After the temperature reaches 250 K, the intensity at the $(0\frac{2}{3})$ position starts decreasing as shown in Fig. 7. However, the behavior of the temperature-intensity curves for the $(0\frac{1}{2})$ position is dependent on the coverage. In Fig. 7(a), at low coverage ($\Theta=0.1$) the transition is one in which the streak pattern becomes stable at $T_{(LR)}\simeq 250$ K. The inensities at the $(0\frac{1}{2})$ and $(0\frac{2}{3})$ positions are both decreasing due to the Debye-Waller effect. In Figs. 7(b) and 7(c), at $\Theta=0.18$ and $\Theta=0.22$, respectively, the streak pattern goes to a long-range-ordered (1×2) structure at $T_{(1\times2R)}$. The LEED intensity at the $(0\frac{2}{3})$ position starts decreasing and the intensity at $(0\frac{1}{2})$ is still increasing with temperature until $T_{(W1\times2R)}\simeq 340$ K at which a stable (1×2) reconstruction is reached. Within the temperatures between $T_{(1\times2R)}$ and $T_{(W1\times2R)}$, a significant decrease in the $(0\frac{1}{2})$ beam width has been also observed as the intensity of the $(0\frac{1}{2})$ beam increases in Figs. 7(b) and 7(c). At temperatures below $T_{(W1\times2R)}$, the (1×2) reconstructed structure is, therefore, not well long-range ordered and possibly similar to the "(5×2)"-like domain structure proposed for the (1×2) reconstructed Ni(110) surface.[9] AES measurements have further confirmed that the increase of the $(0\frac{1}{2})$ beam intensity in Figs. 7(b) and

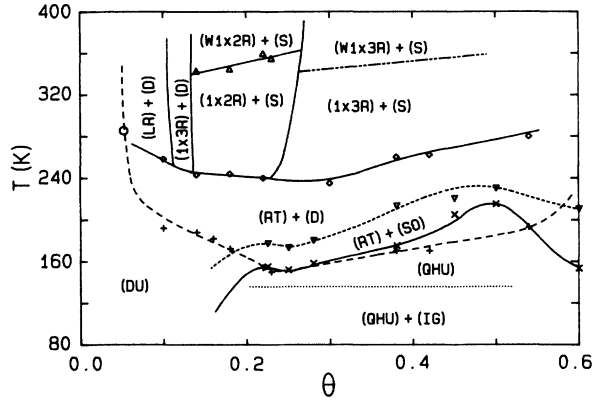

FIG. 8. The phase diagram of the cesium overlayer and substrate reconstructed phase for Cs on Cu(110). (QHU)=(QH), the quasihexagonal structure overlayer on the unreconstructed substrate. (IG)=the immobile gas in the quasihexagonally ordered overlayer. (DU)=disordered cesium on the unreconstructed substrate. (RT)=reconstruction phase transition region. (SO)=a short-range-ordered quasihexagonal overlayer. (D)=disordered adatoms on the reconstructed substrate. (S)=the additional streaks in the diffraction pattern from the overlayer. (LR)=the local substrate reconstruction. $(1\times2R)$=a (1×2) reconstructed substrate. $(W1\times2R)$=a well-ordered (1×2) reconstructed substrate. $(1\times3R)$=a (1×3) reconstructed substrate. $(W1\times3R)$=a well-ordered (1×3) substrate reconstruction. (QHR)=a quasihexagonally ordered overlayer on the (1×3) reconstructed substrate.

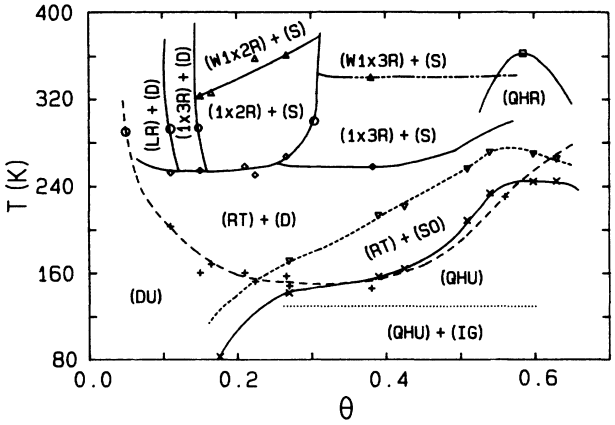

FIG. 9. The phase diagram of the potassium overlayer and substrate reconstructed phases for K on Cu(110). Notations are the same as those in Fig. 8.

7(c) at $T>250$ K are not related to thermal desorption of Cs. The disappearance of the (1×2) phase at $T\simeq 700$ K, however, results from thermal desorption of the alkali adatoms since a major reduction of the adatom AES signal has been observed for $T>500$ K.

At higher cesium coverages ($\Theta>0.3$), the streak pattern [Fig. 5(a)] also appears at $T\simeq 160$ K and goes to the (1×3) phase at $T>260$ K. The (1×3) structure can be improved by warming up to $T\simeq 320$ K and cooling down.

The Cu(110) surface reconstruction induced by potassium is very similar to that induced by cesium discussed earlier in this paper. The differences are only in the values of the transition temperatures and coverage, as will be seen in the following discussion on the K and Cs surface phase diagrams.

C. Phase diagrams of K and Cs on the Cu(110) surface

The phase diagrams for Cs and K shown in Figs. 8 and 9 are derived from compilation of all of the LEED measurements and observations for K and Cs on the Cu(110) surface and show the relationship between the ordered

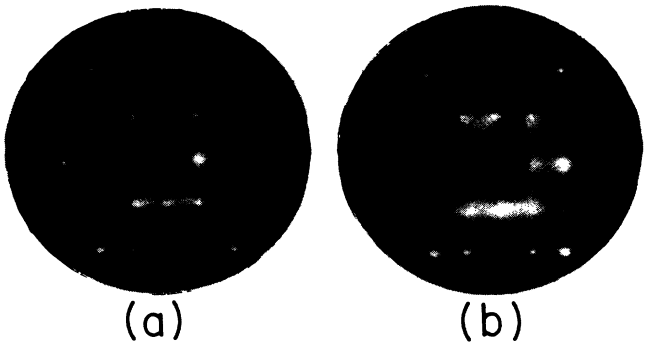

FIG. 10. LEED patterns of the $p(2\times2)$-like phase on the 80 K-Cu(110) substrate at a coverage of $\Theta\simeq 0.25$, (a) for a Cs overlayer and (b) for a K overlayer.

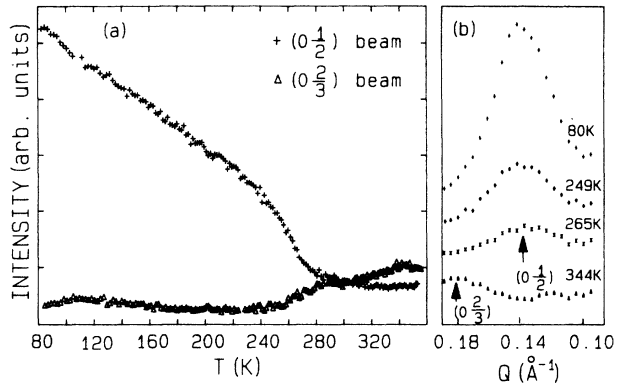

FIG. 11. LEED intensities and beam profiles of the $(0\frac{1}{2})$ beam and the $(0\frac{2}{3})$ beam as a function of temperature for the structure shown in Fig. 10 with excess cesium coverage $\Theta \simeq 0.2$. $\Delta\Theta$ is the extra amount of the alkali-metal coverage evaporated onto the well-ordered (1×2) reconstructed phase at 80 K.

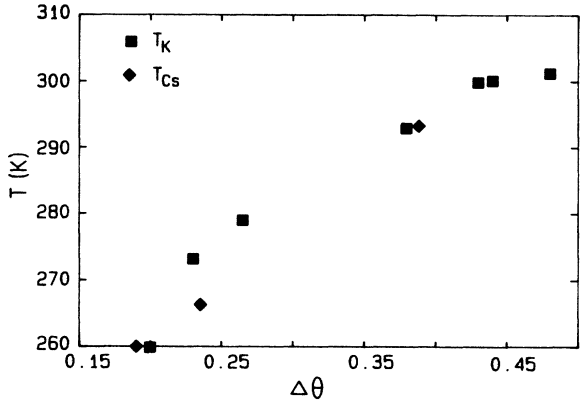

FIG. 12. The transition temperature of a (1×2) reconstructed phase to a (1×3) phase as a function of excess alkali-metal coverage $\Delta\Theta$.

overlayer phases and the substrate reconstruction phases. The data points indicated in Figs. 8 and 9 are obtained from the measurements of the intensity-temperature and the FWHM-temperature behavior of the diffraction features, except those defined by circles, which come from careful observations of LEED patterns. The phase diagrams for K and Cs are quite similar. Both diagrams show the minimum substrate reconstruction transition temperatures in the form of bowl shaped dashed curves, and a wide reconstruction transition region in which the intensities of the streaks in the diffraction patterns [Fig. 5(a)] are increasing with increase in temperature.

It is quite clear that the disordering transition temperature of the QH overlayer at $\Theta \simeq 0.4$ is followed by surface reconstruction. The local reconstructed surface can only support a short-range-ordered quasihexagonal overlayer, whereas the (1×3) reconstructed surface can still support the QH potassium overlayer until 360 K at $\Theta \simeq 0.5$, but not support the QH cesium overlayer. The minimum temperature to obtain a well-ordered (1×2) reconstructed surface induced by cesium is about 20 K above that induced by potassium (320 K), although the melting temperature of bulk potassium is about 30 K higher than that of bulk cesium. The QH disordering transition of the overlayers and the substrate surface reconstruction are all irreversible.

D. K and Cs on a well-ordered Cu(110)-(1×2) surface

The K and Cs on the Cu(110) surface at $\Theta > 0.15$ produce well-ordered (1×2) phases with additional diffraction streaks at $T > 320$ K as previously discussed. At $\Theta \simeq 0.2$, after cooling down the sample, the "streaks" break up into a $p(2\times2)$ modulation with a $p(2\times2)$-like phase appearing at $T < 120$ K as shown in Fig. 10. This results from the alkali-adatoms ordering between the "rows" in Fig. 6. A further deposition of K or Cs onto the $p(2\times2)$-like phase overlayer on the 80 K well-ordered (1×2) reconstructed surface results in a position change of the diffracted beams, indicating overlayer interatomic spacing compression. With increase of temperature, the $p(2\times2)$-like phase returns to the (1×2) pattern with the streaks at about 120 K. Further increase in temperature results in the (1×2) phase going to a (1×3) phase at $T > 260$ K.

Figure 11 shows the beam intensities and profiles versus temperature, describing the phase transition from the (1×2) phase to the (1×3) phase. The intensity of $(0\frac{1}{2})$ beam decreases continuously and the intensity at $(0\frac{2}{3})$ increases gradually at $T \simeq 260$ K. The transition temperature from the (1×2) phase to the (1×3) phase is defined as an inflection point in the intensity-temperature curve of $(0\frac{1}{2})$ beam in Fig. 11. As shown in Fig. 12, this transition temperature increases as the deposition, and therefore excess coverage $(\Delta\Theta)$ increases.

IV. CONCLUSIONS

The growth of quasihexagonal (QH) ordered alkali-metal (K and Cs) overlayers on the Cu(110) surface has been observed at 80 K. As coverage was increased, the overlayer interatomic spacings compressed continuously from about 8.5 Å to up to 10% smaller than the bulk interatomic spacing. The continuous order-disorder transitions of the QH overlayers are followed by an alkali-induced local surface reconstruction transition at $T \geq 150$ K. At the temperatures above 320 K and at coverages $\Theta < 0.3$, the reconstruction orders to a well-ordered (1×2) structure. With additional coverage $(\Delta\Theta > 0.2)$, a phase transition takes the (1×2) reconstruction to the (1×3) reconstruction at $T > 260$ K. Phase diagrams detail the surface phase relation for both K and Cs on the Cu(110) surface.

ACKNOWLEDGMENT

Partial support of this work by the R. A. Welch Foundation and NASA is gratefully acknowledged.

[1]G. Kleinle, V. Penka, R. J. Behm, G. Ertl, and W. Moritz, Phys. Rev. Lett. **58**, 148 (1987).
[2]U. Dobler, K. Baberschke, D. D. Vvedensky, and J. B. Pendry, Surf. Sci. **178**, 679 (1986).
[3]W. Moritz and D. Wolf, Surf. Sci. **163**, L655 (1985); **88**, L29 (1979).
[4]J. W. Chung, S. C. Ying, and P. J. Estrup, Phys. Rev. Lett. **56**, 749 (1986).
[5]M. Altman, J. W. Chung, P. J. Estrup, J. M. Kosterlitz, J. Prybyla, D. Sahu, and S. C. Ying, J. Vac. Sci. Technol. A **5**, 1045 (1987).
[6]J. A. Prybyla, P. J. Estrup, S. C. Ying, Y. J. Chabal, and S. B. Christman, Phys. Rev. Lett. **58**, 1877 (1987).
[7]S. E. Trullinger and S. L. Cunningham, Phys. Rev. Lett. **30**, 913 (1973).
[8]M. S. Daw and S. M. Foiles, J. Vac. Sci. Technol. A **4**, 1412 (1986).
[9]Y. Kuk, P. J. Silverman, and H. Q. Nguyen, Phys. Rev. Lett. **59**, 1452 (1987).
[10]B. E. Hayden, K. C. Price, Davie, G. Paolucci, and A. M. Bradshaw, Solid State Commun. **48**, 325 (1983).
[11]A. Ignatiev and W. C. Fan, J. Vac. Sci. Technol. A **4**, 1415 (1986).
[12]W. C. Fan and A. Ignatiev, Phys. Rev. B **37**, 5274 (1988).
[13]W. C. Fan and A. Ignatiev, J. Vac. Sci. Technol. (to be published).
[14]R. L. Gerlach and T. N. Rhodin, Surf. Sci. **17**, 32 (1969).
[15]D. K. Flynn, K. D. Jamison, P. A. Thiel, G. Ertl, and R. J. Behm, J. Vac. Sci. Technol. A **5**, 794 (1987).
[16]M. Jaubert, A. Glachant, M. Bienfait, and G. Boato, Phys. Rev. Lett. **46**, 1679 (1981).
[17]W. Berndt, J. Vac. Sci. Technol. A **5**, 711 (1987).
[18]P. J. Estrup and R. A. Barker, in *Ordering in Two Dimensions*, edited by S. K. Sinha (North-Holland, New York, 1980), p. 39.
[19]R. Dohl-Oelze, E. M. Stuve, and J. K. Sass, Solid State Commun. **57**, 323 (1986).

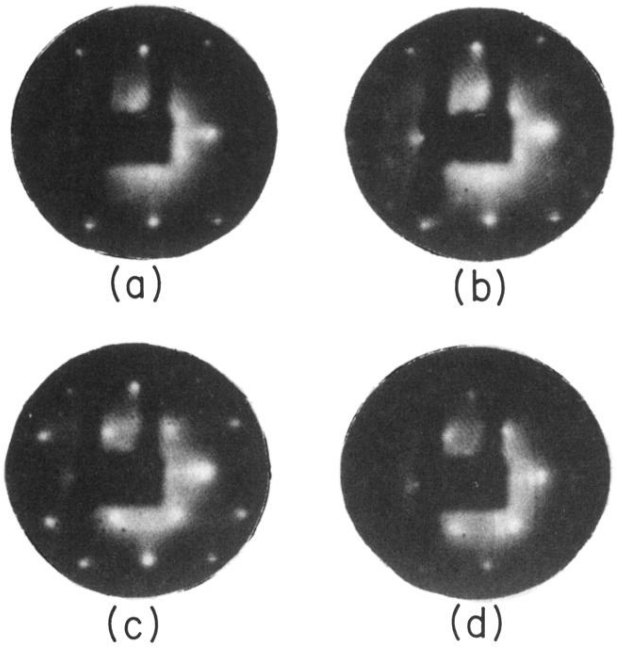

FIG. 1. LEED patterns of the quasihexagonal structure phase (QH) of potassium on the 80-K Cu(110) surface at $E=82$ eV except (d) at $E=84$ eV. (a) $\Theta=0.20$; (b) $\Theta=0.25$; (c) $\Theta=0.50$; (d) $\Theta=0.6$. (d) is the pattern for the minimal K interatomic spacing.

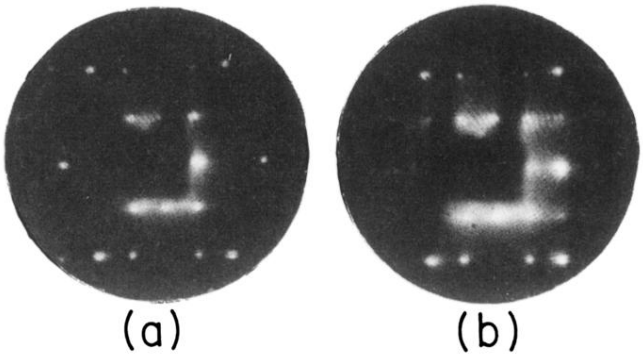

FIG. 10. LEED patterns of the $p(2\times2)$-like phase on the 80 K-Cu(110) substrate at a coverage of $\Theta\simeq0.25$, (a) for a Cs overlayer and (b) for a K overlayer.

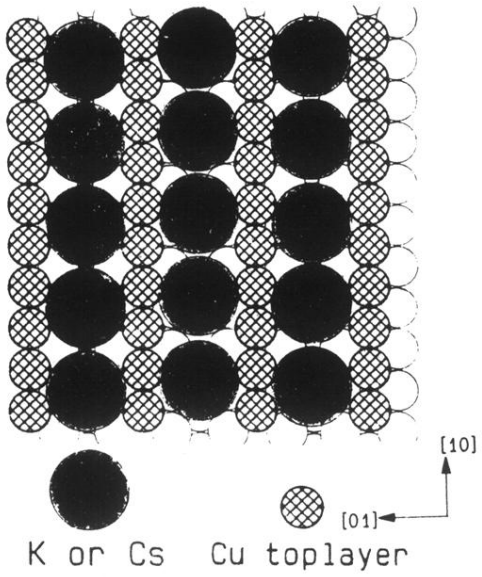

FIG. 6. A possible structure for the (1×2) LEED pattern with additional streaks [Fig. 5(d)], with a (1×2) "missing-row" reconstructed surface and a "row" structure of the alkali-metal overlayer.